

## Fundamental Constants and Tests of Theory in Rydberg States of Hydrogenlike Ions

Ulrich D. Jentschura,<sup>1,2</sup> Peter J. Mohr,<sup>1</sup> Joseph N. Tan,<sup>1</sup> and Benedikt J. Wundt<sup>2</sup>

<sup>1</sup>National Institute of Standards and Technology, Gaithersburg, Maryland 20899-8420, USA

<sup>2</sup>Max-Planck-Institut für Kernphysik, Saupfercheckweg 1, 69117 Heidelberg, Germany

(Received 30 November 2007; published 22 April 2008)

A comparison of precision frequency measurements to quantum electrodynamics (QED) predictions for Rydberg states of hydrogenlike ions can yield information on values of fundamental constants and test theory. With the results of a calculation of a key QED contribution reported here, the uncertainty in the theory of the energy levels is reduced to a level where such a comparison can yield an improved value of the Rydberg constant.

DOI: [10.1103/PhysRevLett.100.160404](https://doi.org/10.1103/PhysRevLett.100.160404)

PACS numbers: 06.20.Jr, 12.20.Ds, 31.15.-p, 31.30.jf

Quantum electrodynamics (QED) makes extremely accurate predictions despite the “mathematical inconsistencies and renormalized infinities swept under the rug” [1]. With the assumption that the theory is correct, it is used to determine values of the relevant fundamental constants by adjusting their values to give the best agreement with experiments [2]. In this Letter, we consider the possibility of making such comparisons of theory and experiment for Rydberg states of cooled hydrogenlike ions using an optical frequency comb. We find that because of simplifications in the theory that occur for Rydberg states, together with the results of a calculation reported here, the uncertainty in the predictions of the energy levels is dominated by the uncertainty in the Rydberg constant, the electron-nucleus mass ratio, and the fine-structure constant. Apart from these sources of uncertainty, to the extent that the theory remains valid, the predictions for the energy levels appear to have uncertainties as small as parts in  $10^{17}$  in the most favorable cases.

The CODATA recommended value of the Rydberg constant has been obtained primarily by comparing theory and experiment for 23 transition frequencies or pairs of frequencies in hydrogen and deuterium [2]. The theoretical value for each transition is the product of the Rydberg constant and a calculated factor based on QED that also depends on other constants. While the most accurately measured transition frequency in hydrogen ( $1S-2S$ ) has a relative uncertainty of  $1.4 \times 10^{-14}$  [3], the recommended value of the Rydberg constant has a larger relative uncertainty of  $6.6 \times 10^{-12}$  which is essentially the uncertainty in the theoretical factor. The main source is the uncertainty in the charge radius of the proton with additional uncertainty due to uncalculated or partially calculated higher-order terms in the QED corrections. This uncertainty could be reduced by a measurement of the proton radius in muonic hydrogen [4], or by a sufficiently accurate measurement of a different transition in hydrogen. On the other hand, for Rydberg states, the fact that the wave function is small near the nucleus results in the finite nuclear size correction being completely negligible. Also, for Rydberg states, the higher-order terms in the QED corrections are relatively

smaller than they are for  $S$  states, so theoretical expressions with a given number of terms are more accurate.

Circular Rydberg states of hydrogen in an 80 K atomic beam have been studied with high precision for transition wavelengths in the millimeter region, providing a determination of the Rydberg constant with a relative uncertainty of  $2.1 \times 10^{-11}$  [5,6]. With the advent of optical frequency combs [7], precision measurements of optical transitions between Rydberg states have now become possible using femtosecond lasers. An illustration is the laser spectroscopy of antiprotonic helium [8]. Figure 1 gives isofrequency curves corresponding to the spacing between adjacent Bohr energy levels ( $n$  to  $n-1$ ) in the two-dimensional parameter space of the principal quantum number  $n$  and the nuclear charge  $Z$  for hydrogenlike ions. Much of this space is accessible to optical frequency synthesizers based on mode-locked femtosecond lasers, which readily provide ultraprecise reference rulers spanning the near-infrared and visible region of the optical spectrum (530–2100 nm). Diverse techniques in spectroscopy (such as double-resonance methods) broaden the range of applications. Even when the absolute accuracy is limited by the primary frequency standard (a few parts in

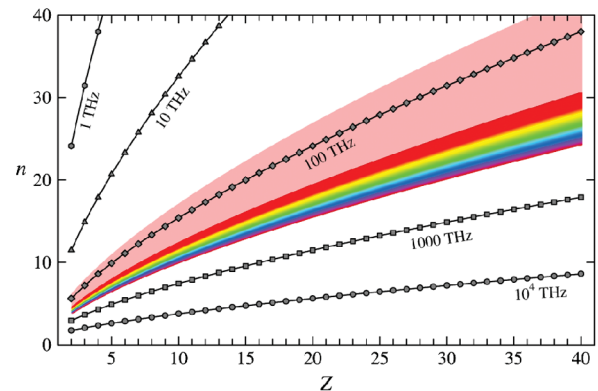


FIG. 1 (color). Graph showing values of  $Z$  and approximate  $n$  that give a specified value of the frequency for transitions between states with principal quantum number  $n$  and  $n-1$  in a hydrogenlike ion with nuclear charge  $Z$ . Frequencies in the near-infrared and visible range are indicated in color.

$10^{16}$ ), optical frequency combs can enable relative frequency measurements with uncertainties approaching 1 part in  $10^{19}$  over 100 THz of bandwidth [9]. The precise pulse train from a femtosecond laser can also be used directly to probe the global atomic structure, thus integrating the optical, terahertz, and radio-frequency domains [10].

There are simplifications in the theory of energy levels of Rydberg states of hydrogenlike ions that, in some cases, allow calculations to be made at levels of accuracy comparable to these breakthroughs in optical metrology. In the following, we write the known theoretical expressions for the energy levels of these ions, describe and give results of a calculation that eliminates the largest source of uncertainty, and list the largest remaining sources of uncertainty. We also make numerical predictions for a transition in two different ions as illustrations, look at the natural linewidth, and discuss what might be learned from comparison of theory and experiment.

In a high- $n$  Rydberg state of a hydrogenlike atom with nuclear charge  $Z$  and angular momentum  $l = n - 1$ , the probability of the electron being within a short distance  $r$  from the origin is of order  $(2Zr/na_0)^{2n+1}/(2n+1)!$ , where  $a_0$  is the Bohr radius. Because of this strong damping near the origin, effects arising from interactions near or inside the nucleus are negligible, including the effect of the finite size of the nucleus.

For  $l \geq 2$ , the theoretical energy levels can be accurately expressed as a sum of the Dirac energy with nuclear motion corrections  $E_{\text{DM}}$ , relativistic-recoil corrections  $E_{\text{RR}}$ , and radiative corrections  $E_{\text{QED}}$ :  $E_n = E_{\text{DM}} + E_{\text{RR}} + E_{\text{QED}}$ . Reviews of the theory and references to original work are given in [2,11,12]. The difference between the Dirac eigenvalue and the electron rest energy is proportional to

$$\alpha^2 D = \left[ 1 + \frac{(Z\alpha)^2}{(n-\delta)^2} \right]^{-1/2} - 1, \quad (1)$$

$$D = -\frac{Z^2}{2n^2} + \left( \frac{3}{8n} - \frac{1}{2j+1} \right) \frac{Z^4 \alpha^2}{n^3} + \dots,$$

where  $\alpha$  is the fine-structure constant,  $\delta = |\kappa| - \sqrt{\kappa^2 - (Z\alpha)^2}$ ,  $\kappa = (-1)^{l+j+1/2}(j+1/2)$  is the Dirac spin-angular quantum number, and  $j$  is the total angular momentum quantum number. The energy level, taking into account the leading nuclear motion effects, but not including the electron or nucleus rest energy, is given by [12]

$$E_{\text{DM}} = 2hcR_\infty \left[ \mu_r D - \frac{r_N \mu_r^3 \alpha^2}{2} D^2 + \frac{r_N^2 \mu_r^3 Z^4 \alpha^2}{2n^3 \kappa (2l+1)} \right], \quad (2)$$

where  $h$  is the Planck constant,  $c$  is the speed of light,  $R_\infty = \alpha^2 m_e c / 2h$  is the Rydberg constant,  $r_N = m_e / m_N$  is the electron-nucleus mass ratio, and  $\mu_r = 1/(1+r_N)$  is the ratio of the reduced mass to the electron mass.

Relativistic corrections to Eq. (2) associated with motion of the nucleus are classified as relativistic-recoil corrections. For the states with  $l \geq 2$  considered here

$$E_{\text{RR}} = 2hcR_\infty \frac{r_N Z^5 \alpha^3}{\pi n^3} \left\{ \mu_r^3 \left[ -\frac{8}{3} \ln k_0(n, l) - \frac{7}{3l(l+1)(2l+1)} \right] + \pi Z\alpha \left[ 3 - \frac{l(l+1)}{n^2} \right] \times \frac{2}{(4l^2-1)(2l+3)} + \dots \right\}, \quad (3)$$

where  $\ln k_0(n, l)$  is the Bethe logarithm. We assume that the uncertainty due to uncalculated higher-order terms is  $Z\alpha \ln(Z\alpha)^{-2}$  times the contribution of the last term in Eq. (3).

Quantum electrodynamics (QED) corrections for high- $l$  states are summarized as

$$E_{\text{QED}} = 2hcR_\infty \frac{Z^4 \alpha^2}{n^3} \left\{ -\mu_r^2 \frac{a_e}{\kappa(2l+1)} + \mu_r^3 \frac{\alpha}{\pi} \left[ -\frac{4}{3} \ln k_0(n, l) + \frac{32}{3} \frac{3n^2 - l(l+1)}{n^2} \right] \times \frac{(2l-2)!}{(2l+3)!} (Z\alpha)^2 \ln \left[ \frac{1}{\mu_r (Z\alpha)^2} \right] + (Z\alpha)^2 G(Z\alpha) \right\}, \quad (4)$$

where  $a_e$  is the electron magnetic moment anomaly and  $G(Z\alpha)$  is a function that contains higher-order QED corrections. Equation (4) contains no explicit vacuum polarization contribution because of the damping of the wave function near the origin. Also in that equation, the uncertainties in the theory of  $a_e$  may be eliminated by using the experimental value  $a_e = 1.159\,652\,180\,73(28) \times 10^{-3}$  obtained with a one-electron quantum cyclotron [13].

The leading terms in  $G(Z\alpha)$  are expected to be

$$G(Z\alpha) = A_{60} + A_{81} (Z\alpha)^2 \ln(Z\alpha)^{-2} + A_{80} (Z\alpha)^2 + \dots + \frac{\alpha}{\pi} B_{60} + \dots + \left( \frac{\alpha}{\pi} \right)^2 C_{60} + \dots \quad (5)$$

The coefficients indicated by the letter  $A$  arise from the one-photon QED corrections;  $A_{60}$  and  $A_{81}$  arise from the self-energy, and  $A_{80}$  arises from both the self-energy and the long-range component of the vacuum polarization. The term  $A_{60}$  has been calculated for many states with  $l \leq 8$ , but not for higher- $l$  states before this work. The uncertainty introduced by this term if it were not calculated, based on plausible extrapolations from lower- $l$  known values, would be the largest uncertainty in the theory and larger than the uncertainty from the Rydberg constant. The higher-order coefficient  $A_{81}$  and the self-energy component of the coefficient  $A_{80}$  are not known, but can be expected to be small. The vacuum polarization contribution to  $A_{80}$  is known [14] and is extremely small. The coefficient  $B_{60}$  arises from two-photon diagrams and has not been calculated for high- $l$  states, but a comparison of calculated values of  $B_{60}$  [15] and  $A_{60}$  [16] for  $l \leq 5$ , suggests it has a magnitude

of roughly  $4A_{60}$ , which is used as the associated uncertainty. Further, a term proportional to  $(\alpha/\pi)B_{61}\ln(Z\alpha)^{-2}$ , that is nonzero for  $S$  and  $P$  states, vanishes for higher- $l$  states [17]. The term  $C_{60}$  is expected to be the next three-photon term, in analogy with the two-photon terms.

In order to eliminate the main source of theoretical uncertainty in the energy levels, we have calculated the value of  $A_{60}$  for a number of Rydberg states. This calculation uses methods from field theory, i.e., nonrelativistic QED (NRQED) effective operators which facilitate the calculation [18], and methods from atomic physics to handle the extensive angular momentum algebra in the higher-order binding corrections of near-circular Rydberg states. Distinct contributions to the self-energy from high- and low-energy virtual photons, are matched using an intermediate cutoff parameter [19]. For near-circular Rydberg states, the radial wave functions have at most a few nodes, yet the calculation of  $A_{60}$  coefficients for these states is much more involved than for low-lying states. The reason is that in using the Sturmian decomposition of the hydrogen Coulomb Green function, as done for lower- $n$  states, the radial integrations lead to sums over hypergeometric functions with high indices, which in turn give rise to an excessive number of terms. For states with  $n = 8$ , there are of order  $10^5$  terms in intermediate steps, which is roughly 2 orders of magnitude more terms than for states with  $n = 2$  [20]. This trend continues as  $n$  increases making calculation at high  $n$  with this conventional method intractable.

Here we report that the calculation has been done with a combined analytic and numerical approach based on lattice methods by using a formulation of the Schrödinger-Coulomb Green function on a numerical grid [21]. Provided quadruple precision ( $\sim 32$  significant digits) in the Fortran code is used, and provided a large enough box to represent the Rydberg states on the grid is used, the positive continuum of states can be accurately represented by a pseudospectrum of states with positive discrete energies. With this basis set, the virtual photon energy integration can be carried out analytically for each pseudostate using Cauchy's theorem. This solves the problem of the calculation of the relativistic Bethe logarithms without the need for the subtraction of many pole terms, which would otherwise be necessary if the virtual photon energy were used as an explicit numerical integration variable. The results of this calculation for a number of states with  $n = 13$  to 16 are given in Table I.

We incorporate the results for  $A_{60}$  to numerically evaluate the theoretical prediction for the frequency of the transition between the state with  $n = 14$ ,  $l = 13$ ,  $j = \frac{27}{2}$  and the state with  $n = 15$ ,  $l = 14$ ,  $j = \frac{29}{2}$  in the hydrogenlike ions  $\text{He}^+$  and  $\text{Ne}^{9+}$ . The constants used in the evaluation are the 2006 CODATA recommended values [22], with the exception of the neon nucleus mass  $m(^{20}\text{Ne}^{10+})$  which is taken from the neon atomic mass [23], corrected for the mass of the electrons and their binding energies. Values of the various contributions and the total are given

TABLE I. Calculated values of the constant  $A_{60}$ . The numbers in parentheses are standard uncertainties in the last figure.

$n$	$l$	$2j$	$\kappa$	$A_{60}$	$2j$	$\kappa$	$A_{60}$
13	11	21	11	$0.679\,575(5) \times 10^{-5}$	23	-12	$4.318\,998(5) \times 10^{-5}$
13	12	23	12	$0.469\,973(5) \times 10^{-5}$	25	-13	$2.729\,475(5) \times 10^{-5}$
14	12	23	12	$0.410\,825(5) \times 10^{-5}$	25	-13	$2.979\,937(5) \times 10^{-5}$
14	13	25	13	$0.296\,641(5) \times 10^{-5}$	27	-14	$1.945\,279(5) \times 10^{-5}$
15	13	25	13	$0.252\,108(5) \times 10^{-5}$	27	-14	$2.116\,050(5) \times 10^{-5}$
15	14	27	14	$0.189\,309(5) \times 10^{-5}$	29	-15	$1.420\,631(5) \times 10^{-5}$
16	14	27	14	$0.155\,786(5) \times 10^{-5}$	29	-15	$1.540\,181(5) \times 10^{-5}$
16	15	29	15	$0.121\,749(5) \times 10^{-5}$	31	-16	$1.059\,674(5) \times 10^{-5}$

as frequencies in Table II. Standard uncertainties are listed with the numbers where they are non-negligible. The theory is sufficiently accurate that the largest uncertainty arises from the Rydberg frequency  $cR_\infty$ , which is a factor in all of the contributions. There is no uncertainty from the Planck constant, since  $\nu = (E_{15} - E_{14})/h$ .

Table III gives sources and estimates of the various known uncertainties in the theory. To put them in perspective, in hydrogen, the relative uncertainty from the two-photon term  $B_{60}$  for the  $1S-2S$  transition is of the order of  $10^{-12}$  due to disagreement between different calculations, whereas in the  $n = 14$  to  $n = 15$  Rydberg transition it is likely to be roughly  $5 \times 10^{-19}$ , based on the smallness of the calculated value of the  $A_{60}$  coefficient. The improved convergence of the expansion of the QED corrections in powers of  $Z\alpha$  is indicated by the fact that  $A_{60}$  is smaller by a factor of about  $10^6$  for the Rydberg states than the value  $A_{60} \approx -30$  for  $S$  states.

The QED level shift given by Eq. (4) is understood to be the real part of the radiative correction, while the complete radiative correction to the level  $\mathcal{E}_{\text{QED}} = E_{\text{QED}} - i\Gamma/2$  is complex and includes an imaginary part proportional to the rate  $A = \Gamma/\hbar$  for spontaneous radiative decay of the level to all lower levels. For the highest- $l$  state with principal quantum number  $n$ , the dominant decay mode is an  $E1$  decay to the highest- $l$  state with principal quantum number  $n - 1$  [24]. Formulas in Ref. [24] give the nonrelativistic expression for the decay rate, which can also be derived from the nonrelativistic limit of the imaginary part of the level shift [25].

As a first approximation, for transitions between states with quantum numbers  $n$  and  $n - 1$  the ratio of the transition energy to the width of the line, is given by

TABLE II. Transition frequencies between the highest- $j$  states with  $n = 14$  and  $n = 15$  in hydrogenlike helium and hydrogenlike neon.

Term	$^4\text{He}^+$ $\nu(\text{THz})$	$^{20}\text{Ne}^{9+}$ $\nu(\text{THz})$
$E_{\text{DM}}$	8.652 370 766 008(58)	216.335 625 5746(14)
$E_{\text{RR}}$	0.000 000 000 000	0.000 000 000 1
$E_{\text{QED}}$	-0.000 000 001 894	-0.000 001 184 1
Total	8.652 370 764 114(58)	216.335 624 3907(14)



TABLE III. Sources and estimated relative standard uncertainties in the theoretical value of the transition frequency between the highest- $j$  states with  $n = 14$  and  $n = 15$  in hydrogenlike helium and hydrogenlike neon.

Source	He <sup>+</sup>	Ne <sup>9+</sup>
Rydberg constant	$6.6 \times 10^{-12}$	$6.6 \times 10^{-12}$
Fine-structure constant	$7.0 \times 10^{-16}$	$1.7 \times 10^{-14}$
Electron-nucleus mass ratio	$5.8 \times 10^{-14}$	$1.2 \times 10^{-14}$
$a_e$	$5.1 \times 10^{-20}$	$1.3 \times 10^{-18}$
Theory: $E_{RR}$ higher order	$6.2 \times 10^{-17}$	$2.4 \times 10^{-14}$
Theory: $E_{QED}A_{81}$	$1.7 \times 10^{-18}$	$1.6 \times 10^{-14}$
Theory: $E_{QED}B_{60}$	$8.6 \times 10^{-18}$	$5.4 \times 10^{-15}$

$$Q = \frac{E_n - E_{n-1}}{\Gamma_n + \Gamma_{n-1}} \rightarrow \frac{3n^2}{4\alpha(Z\alpha)^2} + \dots, \quad (6)$$

where the expression on the right is the asymptotic form as  $n \rightarrow \infty$  of the nonrelativistic value. This is just a rough indication, since transitions with smaller  $l$  values will generally have a smaller  $Q$ , whereas transitions with a change of  $n$  greater than 1 will have a larger  $Q$ . The effect of possible asymmetries of the line shape on the apparent resonance center has been shown to be small by Low [26], of order  $\alpha(Z\alpha)^2 E_{QED}$ . For the  $1S-2S$  transition in hydrogen, such effects are indeed completely negligible at the current level of experimental accuracy [27]. However, for Rydberg states of hydrogenlike ions, particularly at higher- $Z$ , asymmetries in the line shape, some of which depend on details of the experiment, may be significant, and can be calculated if necessary.

Recent advances in atomic-molecular-optical physics have generated an array of tools and techniques useful for engineering highly simplified atomic systems [28]. In particular, observations of cold antihydrogen production at CERN illustrate two ways for a cooled ion/antiproton to capture an electron/positron in high- $l$  Rydberg states, either by three-body recombination or by charge exchange [29]. Properties of atomic cores have also been studied using a double-resonance detection technique to observe the fine structure of Rydberg states produced by charge exchange in a fast beam of highly charged ions [30]. Using electron cooling [29] (and charge exchange), cold hydrogenlike ions can be recombined in high- $l$  Rydberg states from a variety of bare ions extracted from sources such as an electron beam ion source or trap. Although two-photon spectroscopy is possible in certain cases, if the ions are confined in a trap within a region smaller than about half the wavelength of the radiation exciting the transition, Dicke narrowing also eliminates the first-order Doppler shift [31]. Assuming  $T = 100$  K, the relative second-order Doppler shift is about  $3.5 \times 10^{-12}$  for He<sup>+</sup> and  $7 \times 10^{-13}$  for Ne<sup>9+</sup>. Temperatures in the range  $4 \text{ K} < T < 77 \text{ K}$  are obtainable in cryogenic ion traps by resistive cooling [31] and by electron or positron cooling [29]. For lower tem-

peratures ( $T < 1$  K), sympathetic laser cooling methods can be used [31].

Of the variety of  $(n, l, Z)$  combinations of hydrogenlike ions, circular Rydberg states of low- $Z$  ions seem the most favorable for a comb-based determination of the Rydberg constant. On the other hand, some perturbations are smaller and linewidths are larger in heavier ions. Hence, using ions with a variety of  $(n, Z)$  combinations could be useful for experimental optimization and consistency checks, as well as for extending diversity of experiments used to determine fundamental constants and test theory.

U.D.J. and B.J.W. acknowledge support from the Deutsche Forschungsgemeinschaft (Heisenberg program and contract Je285/4-1). Mr. Frank Bellamy provided assistance with some of the numerical evaluations.

- [1] F. Dyson, Letter to G. Gabrielse, July 15 (2006).
- [2] P. J. Mohr and B. N. Taylor, Rev. Mod. Phys. **77**, 1 (2005).
- [3] T. Hänsch *et al.*, Phil. Trans. R. Soc. A **363**, 2155 (2005).
- [4] T. Nebel *et al.*, Can. J. Phys. **85**, 469 (2007).
- [5] D. Kleppner (private communication).
- [6] J. C. De Vries, Ph.D. thesis, MIT, 2001.
- [7] T. W. Hänsch, Rev. Mod. Phys. **78**, 1297 (2006).
- [8] M. Hori *et al.*, Phys. Rev. Lett. **96**, 243401 (2006).
- [9] L.-S. Ma *et al.*, Science **303**, 1843 (2004).
- [10] A. Marian *et al.*, Science **306**, 2063 (2004).
- [11] J. R. Sapirstein and D. R. Yennie, in *Quantum Electrodynamics*, edited by T. Kinoshita (World Scientific, Singapore, 1990), Chap. 12, p. 560.
- [12] M. I. Eides *et al.*, Phys. Rep. **342**, 63 (2001).
- [13] D. Hanneke *et al.*, Phys. Rev. Lett. **100**, 120801 (2008).
- [14] E. H. Wichmann and N. M. Kroll, Phys. Rev. **101**, 843 (1956).
- [15] U. D. Jentschura, Phys. Rev. A **74**, 062517 (2006).
- [16] E.-O. Le Bigot *et al.*, Phys. Rev. A **68**, 042101 (2003).
- [17] U. D. Jentschura *et al.*, Phys. Rev. A **72**, 062102 (2005).
- [18] W. Caswell and G. Lepage, Phys. Lett. B **167**, 437 (1986).
- [19] B. J. Wundt and U. D. Jentschura, Phys. Lett. B **659**, 571 (2008).
- [20] U. D. Jentschura *et al.*, Phys. Rev. Lett. **90**, 163001 (2003).
- [21] S. Salomonson and P. Öster, Phys. Rev. A **40**, 5559 (1989).
- [22] <http://physics.nist.gov/constants>.
- [23] G. Audi *et al.*, Nucl. Phys. A **729**, 337 (2003).
- [24] H. A. Bethe and E. E. Salpeter, *Quantum Mechanics of One- and Two-Electron Atoms* (Academic, New York, 1957).
- [25] U. D. Jentschura *et al.*, J. Phys. B **38**, S97 (2005).
- [26] F. Low, Phys. Rev. **88**, 53 (1952).
- [27] U. D. Jentschura and P. J. Mohr, Can. J. Phys. **80**, 633 (2002).
- [28] AMO2010, *Controlling the Quantum World* (National Academies, Washington, DC, 2007).
- [29] G. Gabrielse, Adv. At. Mol. Opt. Phys. **50**, 155 (2005).
- [30] S. R. Lundeen and C. W. Fehrenbach, Phys. Rev. A **75**, 032523 (2007).
- [31] W. M. Itano *et al.*, Phys. Scr. **T59**, 106 (1995).